Spike protein cleavage-activation mediated by the SARS-CoV-2 P681R mutation: a case-study from its first appearance in variant of interest (VOI) A.23.1 identified in Uganda

Bailey Lubinski [1,2 #], Laura E. Frazier [1,2 #], My V.T. Phan [3], Daniel L. Bugembe [3], Tiffany Tang [4], Susan Daniel [4], Matthew Cotten [3,5], Javier A. Jaimes [2 *] and Gary R. Whittaker [2, 6 *]

[1] Graduate Program in Biological & Biomedical Sciences, Cornell University, Ithaca, NY, 14853, USA.

[2] Department of Microbiology & Immunology, College of Veterinary Medicine, Cornell University, Ithaca, NY, 14853, USA.

[3] MRC/UVRI & London School of Hygiene and Tropical Medicine – Uganda Research Unit, Entebbe, Uganda.

[4] Robert Frederick Smith School of Chemical & Biomolecular Engineering, Cornell University, Ithaca, NY, 14853, USA.

[5] MRC Centre of Virus Research, University of Glasgow, Glasgow, United Kingdom.

[6] Master of Public Health Program, Cornell University, Ithaca, NY, 14853, USA.

[#] Contributed equally

* Corresponding authors

618 Tower Rd., Ithaca NY 14853, USA

jaj246@cornell.edu; grw7@cornell.edu

24

25 **Graphical abstract**

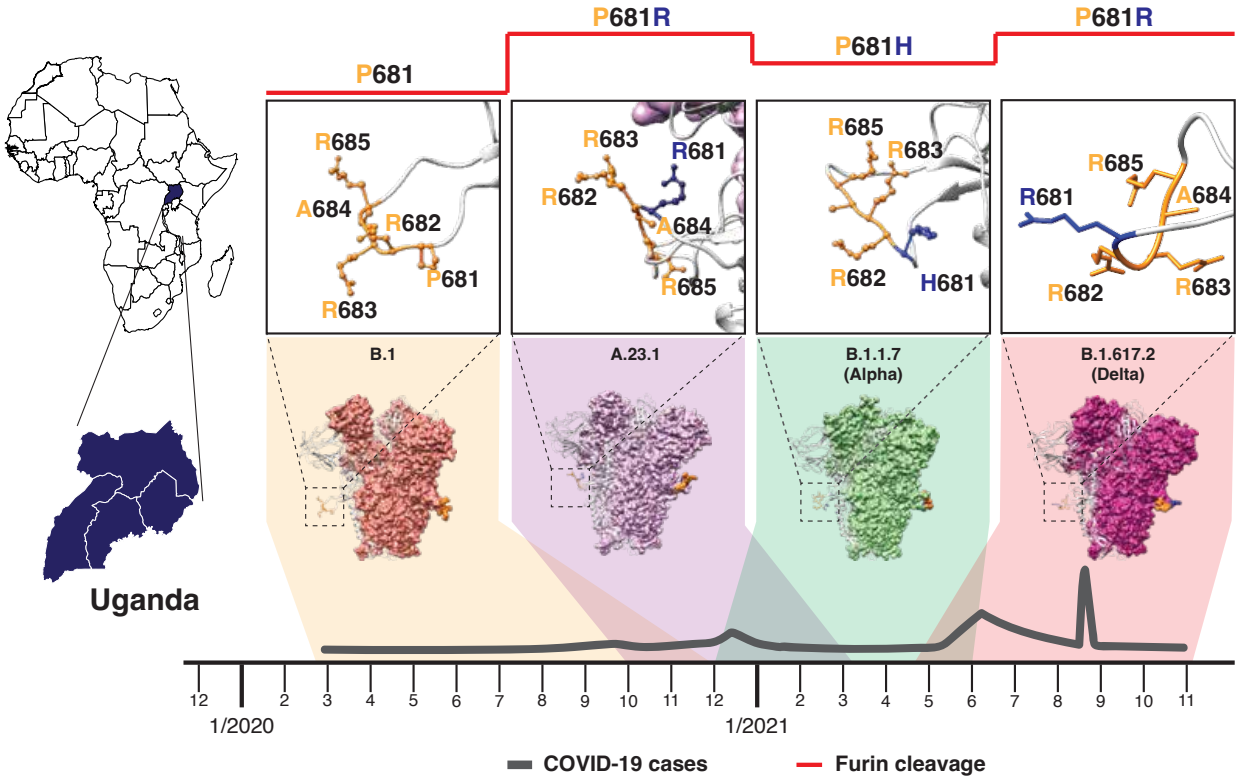

26

27

28 **Abstract**

29 The African continent like all other parts of the world with high infection/low vaccination rates can, and
30 will, be a source of novel SARS-CoV-2 variants. The A.23 viral lineage, characterized by three spike
31 mutations F157L, V367F and Q613H, was first identified in COVID-19 cases from a Ugandan prison in
32 July 2020, and then was identified in the general population with the additional spike mutation P681R at the
33 S1/S2 cleavage site to comprise lineage A.23.1 by September 2020 with subsequent spread to 26 other
34 countries. The P681R spike substitution of A.23.1 is of note as it increases the number of basic residues in
35 the sub-optimal SARS-CoV-2 spike protein furin cleavage site; as such, this substitution may affect viral
36 replication, transmissibility, or pathogenic properties. The same P681R substitution has also subsequently
37 appeared in B.1.617 variants, including B.1.617.2 (Delta). Here, we performed assays using fluorogenic

peptides mimicking the S1/S2 from A.23.1 and B.1.617 and observed significantly increased cleavability with furin, compared to sequences derived from the original Wuhan-Hu1 S1/S2. We performed cell-cell fusion and functional infectivity assays using pseudotyped particles harboring SARS-CoV-2 spike proteins and observed an increase in transduction for A.23.1-pseudotyped particles compared to Wuhan-Hu-1. However, these changes in activity were not reproduced in the original Wuhan-Hu-1 spike bearing only the P681R substitution. Our findings suggest that while A.23.1 has increased furin-mediated cleavage linked to the P681R substitution—which may affect viral infection and transmissibility—this substitution alone needs to occur on the background of other spike protein changes to enable its full functional consequences.

Key words:

SARS-CoV-2, A.23.1 variant, Uganda, spike, P681R mutation

Introduction

Severe acute respiratory syndrome coronavirus 2 (SARS-CoV-2) is the agent causing the current COVID-19 pandemic (1). SARS-CoV-2 was first identified in late 2019 and has since spread rapidly throughout the world. The virus has evolved into two main lineages, A and B and multiple additional lineages. While the B.1 lineage became the dominant virus following its introduction into Northern Italy and spread through Europe/UK in February 2020, both A and B lineages remain in circulation globally (2). Both lineages have undergone significant diversification as they expanded; this expansion is apparently linked to a key S gene mutation—D614G in lineage B.1 and all sublineages, which has been linked to modest increase in virus transmissibility (3) and with Q613H found in lineage A.23/A.23.1. As Q613H is adjacent to D614G it may represent an example of convergent evolution that resulted in a more stabilized spike protein (4). D614G has now become established in circulating B and derived lineages. Compared with the lineage B.1 viruses that have successfully evolved into multiple variants of concern (VOC), including B.1.1.7 (Alpha) B.1.351 (Beta), B.1.1.28.1/P.1 (Gamma), B.1.617.2 (Delta), most of lineage A viruses remained at fairly lower

63 frequency and were more prevalent at the beginning of the pandemic in Asia. However, the A.23.1 viral
64 lineage is one of a few lineage A viruses that, due to local circumstances, became abundant in Uganda (5),
65 Rwanda (6) and South Sudan (7). A.23.1 evolved from the A.23 virus variant first identified in Uganda in
66 July 2020 and is characterized by three spike mutations F157L, V367F and Q613H (8). Subsequently, the
67 evolving A.23.1 lineage acquired additional spike substitutions (P681R), as well as in nsp6, ORF8 and ORF9
68 and with the acquisition of the E484K substitution A.23.1 was designated a variant under investigation
69 (VUI). By July 2021, the A.23.1 lineage has been observed with 1110 genomes reported from 47 countries
70 (GISAID, Pango Lineage report; https://cov-lineages.org/global_report_A.23.1.html).
71 Among several mutations in the A.23.1 lineage, the P681R mutation is of interest as it is part of a proteolytic
72 cleavage site for furin and furin-like proteases at the junction of the spike protein receptor-binding (S1) and
73 fusion (S2) domains (9). The S1/S2 junction of the SARS-CoV-2 S gene has a distinct indel compared to all
74 other known SARS-like viruses (Sarbecoviruses in *Betacoronavirus* lineage B)—the amino acid sequence of
75 SARS-CoV-2 S protein is $_{681}$-P-R-R-A-R|S-$_{686}$ with proteolytic cleavage (|) predicted to occur between the
76 arginine and serine residues depicted. Based on nomenclature established for proteolytic events (10), the
77 R|S residues are defined as the P1|P1' residues for enzymatic cleavage, with residue 681 of A.23.1 spike
78 being the P5 cleavage position. The ubiquitously-expressed cellular serine protease furin is highly specific
79 and cleaves at a distinct multi-basic motif containing paired arginine residues; furin requires a minimal motif
80 of R-x-x-R (P4-x-x-P1), with a preference for an additional basic (B) residue at P2; i.e., R-x-B-R (11). For
81 SARS-CoV-2, the presence of the S1/S2 "furin site" enhances virus transmissibility (12, 13). For the A.23.1
82 S, P681R provides an additional basic residue at P5 and may modulate S1/S2 cleavability by furin, and hence
83 virus infection properties (14). Notably, the P681R substitution appears in several other lineages, most
84 notably B.1.617.2 (Delta)(N = 617590 genomes) but also the AY.X sublineages of B.1.617.2, B.1.617.1 (N=
85 6138), B.1.466.2 (N=2208), the B.1.1.7 sublineage Q.4 (2067), B.1.551 (N=722), AU.2 (N=302), B.1.1.25
86 (N=509), B.1.466.2 (N=538), and other lineages (updated 22 Oct 21, https://outbreak.info;

87 https://outbreak.info/situation-reports?pango&muts=S%3AP681R) suggesting that the substitution may
88 provide an advantage for viruses encoding the substitution.
89 We previously studied the role of proteolytic activation of the spike protein of the lineage B SARS-CoV-2
90 isolates Wuhan-Hu1 and B.1.1.7 (15). Here, we used a similar approach to study the role of the proteolytic
91 activation of the spike protein in the context of the A.23.1 lineage virus, with a focus on the P681R
92 substitution to better understand the role of this notable change at the S1/S2 (furin) cleavage site.
93

94 **Results**

95 **Emergence and analysis of SARS-CoV-2 variants in Uganda**

96 A summary of the daily reported SARS-CoV-2 infections in Uganda is shown in Figure 1A, along with a
97 summary of SARS-CoV-2 lineage data in samples from Uganda (Figure 1B). The peak of infections in
98 December 2020-January 2021 corresponded to the circulation of the A.23.1 variant, which subsided, but
99 was replaced by a second larger peak of infections beginning in July 2021, primarily due to the emergence
100 of the B.1.617.2 variant (Delta), with additional variants being present over time. The circulation of the
101 A.23.1 variant appears to be fully displaced by the B.1.617.2 variant, which by July 2021 became the prevalent
102 variant in this country.
103

104 **Bioinformatic and biochemical analysis of the SARS-CoV-2 A.23.1 S1/S2 cleavage site**

105 Along with other changes in the spike protein, A.23.1, B.1.617.1 (Kappa) and B.1.617.2 (Delta) contain a
106 P681R substitution at the S1/S2 interface (Figure 2A), which may modulate spike protein function based on
107 changes to the furin cleavage site and downstream changes in the levels of cleaved products and in virus-cell
108 fusion activation. To gain insight into proteolytic processing at the S1/S2 site of the SARS-CoV-2 spike
109 protein, we first took a bioinformatic approach utilizing the PiTou (16) and ProP (17) cleavage prediction
110 tools, comparing the spike proteins from A.23.1 to B.1.1.7 and the prototype SARS-CoV-2 from the A.1
111 and B.1 lineages (e.g. Wuhan-Hu-1), as well as to MERS-CoV and selected other human respiratory

112 betacoronaviruses (HCoV-HKU1 and HCoV-OC43) with identifiable furin cleavage sites (Figure 2B). Both
113 algorithms predicted an increase in the furin cleavage for the A.23.1 and B.1.617 lineages compared to
114 A.1/B.1, with PiTou also showing a marked increase compared to B.1.1.7. PiTou utilizes a hidden Markov
115 model specifically targeting 20 amino acid residues surrounding furin cleavage sites and is expected to be
116 more accurate prediction tool. As expected, MERS-CoV showed a relatively low furin cleavage score, with
117 HCoV-HKU1 and HCoV-OC43 showing relatively high furin cleavage scores. Overall, these analyses
118 predict a distinct increase of furin cleavability for the spike protein of A.23.1 and B.1.617 lineage viruses
119 compared to A.1/B.1 and B.1.1.7. lineage viruses.
120 To directly examine the activity of furin on the SARS-CoV-2 A.23.1 S1/S2 site, we used a biochemical
121 peptide cleavage assay to directly measure furin cleavage activity *in vitro* (18). The specific peptide sequences
122 used here were SARS-CoV-2 S1/S2 B.1.1.7 (TNSHRRARSVA), TNSPRRARSVA (Wuhan-Hu-1 S1/S2)
123 and TNSRRRARSVA (A.23.1 S1/S2). As predicted, furin effectively cleaved both the Wuhan-Hu-1 (WT)
124 and B.1.1.7 peptides, but with no significant differences (Figure 2C). Interestingly, and agreeing with the
125 PiTou prediction, we observed a significant increase in furin cleavage for the A.23.1 S1/S2 peptide (Figures
126 2B and C) compared to both Wuhan-Hu-1 (WT) and B.1.1.7. This comparative data with SARS-CoV S1/S2
127 sites reveals that the P618R substitution substantially increases cleavability by furin, beyond the small
128 increase noted previously for P681H (12).
129
130 **Cell-to-cell fusion assays of A.23.1 spike**
131 In order to assess the functional properties of the spike protein and to see if the P681R substitution provided
132 any advantage for cell-to-cell transmission or syncytia formation, we performed a cell-to-cell fusion assay in
133 which VeroE6 or Vero-TMPRSS2 cells were transfected with either the WT, A.23.1 or P681R spike gene.
134 We then evaluated syncytia formation as a read-out of membrane fusion. We observed an increase in the
135 syncytia formation following spike protein expression for either A.23.1 or Wuhan-Hu-1 harboring a P681R
136 mutation (P681R), compared to Wuhan-Hu-1 (WT) (Figure 3A). Vero-TMPRSS2 cells generally formed

137 more extensive syncytia than VeroE6 cells, with similar trends observed. This increase was evident by
138 observation through fluorescence microscopy, as well as by quantification of the syncytia and cell-to-cell
139 fusion ratio (Figure 3A, B and C). An increase in the number of nuclei involved in syncytia was observed in
140 cells transfected with A.23.1 and P681R S genes in both cell lines (Figure 3B). However, the increase was
141 higher in Vero-TMPRSS2 cells. We also observed an increase in the cell-to-cell fusion ratio (quantified by
142 fluorescence intensity) in A.23.1 and P681R spike transfected cells, compared to WT (Figure 3C) and as with
143 the previous analysis, the ratio was higher in Vero-TMPRSS2 cells. Membrane expressed spike cleavage also
144 assessed using western blot (Figure 3D). An increased cleavage ratio was observed in the A.23.1 and P681R
145 membrane expressed spikes, compared to WT. Interestingly, the cleavage ratio was similar in both cell lines.
146 Band intensity was normalized to the GLUT4 protein (housekeeping protein) band intensity. These data
147 provide evidence that the P681R mutation increases membrane fusion activity of the SARS-CoV-2 spike
148 protein under the conditions tested.
149
150 **Functional analysis of virus entry using viral pseudoparticles**
151 To assess the functional importance of the S1/S2 site for SARS-CoV-2 entry, we utilized viral
152 pseudoparticles consisting of a murine leukemia virus (MLV) core displaying a heterologous viral envelope
153 protein to partially recapitulate the entry process of the native coronavirus. The pseudoparticles also contain
154 a luciferase reporter gene as well as the integrase activity to allow that integration into the host cell genome
155 to drive expression of quantifiable luciferase (MLVpp-SARS-CoV-2 S) (19). Using the HEK-293T cell line
156 for particle production, MLV pseudoparticles containing the spike proteins of A.23.1, Wuhan-Hu-1 SARS-
157 CoV-2 (WT), and a P681R point mutant of Wuhan-Hu-1 (P681R) were prepared. Positive-control particles
158 containing the vesicular stomatitis virus (VSV) G protein and negative-control particles (Δenvpp) lacking
159 envelope proteins were also prepared (not shown). The pseudoparticles were probed for their S content via
160 western blot (Figure 4A). Because SARS-CoV-S has an efficiently cleaved spike we also produced particles
161 under furin inhibition, using dec-RVKR-CMK which has previously shown to be effective inhibiting furin

162 and other proprotein convertases. This allows changes in cleavage patterns between different spike proteins
163 to be visualized. We also treated the particles with exogenous furin (+ or – furin) to examine the spike
164 cleavage on both partially cleaved and uncleaved spikes, to further study the differences in furin processing
165 in the studied spikes. For both A.23.1 and P681R particles, we detected increased spike protein cleavage
166 compared to WT in the harvested particles (Figure 4A). Interestingly, we observed markedly increased
167 cleavage ratio for both A.23.1 and P681R spikes in the harvested pseudoparticles under furin-inhibition
168 conditions (Figure 4A).
169 We next examined the infection properties of SARS-CoV-2 pseudoparticles in cell lines representative of
170 both the "early" and "late" cell entry pathways (Figure 4B). Furin is predicted to cleave during virus assembly
171 and "prime" the spike protein at the S1/S2 site for subsequent events during cell entry. However, a
172 subsequent cleavage priming at a secondary site (known as S2' site) is also needed to activate the spike's
173 fusion machinery (1). SARS-CoV-2 is predicted to enter Vero E6 cells using cathepsin L for S2' priming
174 during endosomal trafficking, in what is known as the "late" pathway, whereas in Vero-TMPRSS2 is
175 predicted to use a "early" pathway, with the spike's S2' site being activated by TMPRSS2 or other
176 transmembrane serine proteases (TTSPs) at the cellular membrane. (1). Specifically, we used the Vero-
177 TMPRSS2 ("early pathway") and the Vero E6 ("late pathway") cell lines, which are predicted to activate the
178 SARS-CoV-2 S2' using TMPRSS2 and cathepsin L respectively. Considering that furin priming at the S1/S2
179 site normally occurs during viral assembly, we used pseudoparticles that were produced without furin
180 inhibitor, yielding cleaved spike proteins. Vero-TMPRSS2 cells gave overall significantly higher luciferase
181 signal indicative of more efficient entry. In contrast, we observed lowered infection in Vero E6 cells. As
182 expected, VSVpp (positive control) pseudoparticles infected both cell lines with several orders of magnitude
183 higher luciferase units than the values reported with Δenvpp infection (data not shown).
184
185 **Evolution of the P681R mutation and its role in the transmissibility and emergence of SARS-CoV-**
186 **2**

187 To further understand the evolution of the P681R substitution and its role in the transmissibility of SARS-
188 CoV-2, we monitored the frequency of substitutions at the S1/S2 (furin cleavage) site in the global
189 surveillance data and plotted these substitution data as fraction of total genomes. The initial B lineage virus
190 that spread out of Wuhan encoded a spike protein with P681 at the furin cleavage site, along with G614.
191 Fairly early in the epidemic, the D614G substitution appeared in the B.1 lineage and became prevalent in
192 May-December 2020 (Figure 5A). The B.1.1.7 (Alpha) lineage evolved from B.1, spread widely in the UK
193 and other regions and encoded a P681H substitution in the G614D background. B.1.1.7 peaked globally in
194 March-April 2021 (Figure 5A). In most regions of the world, the B.1.617.2 (Delta) lineage encoding spike
195 D614G and P681R spread widely following its emergence in India in May-June 2021, and became the
196 dominant observed lineage globally (Figure 5A). In comparison, a distinct A lineage virus (A.23) containing
197 Q613H appeared in August-September 2020 and acquired the P681R mutation at a much earlier time
198 (December 2020-January 2021); however, it circulated only briefly (Figure 5B).
199

200 **Discussion**

201 Since late 2020, the evolution of the SARS-CoV-2 pandemic has been characterized by the emergence of
202 viruses bearing sets of substitutions/deletions, designated "variants of concern" (VOCs) and "variants under
203 investigation" (VUIs). These variants appear to have expanded following the selection for substitution or
204 deletions in the spike protein, such as D614G and Q613H, along with mutations in other viral proteins. The
205 substitutions encoded by such variants may alter virus characteristics including enhanced transmissibility and
206 antigenicity, some provide a direct advantage to avoid the changing developing immune responses in the
207 population due to prior exposure or vaccination as well as the social dynamics of the human population (4,
208 20-23). The first notable SARS-CoV-2 VOC of 2021 was B.1.1.7 (Alpha), which among other changes,
209 encoded a P681H substitution in the spike S1/S2 furin cleavage site and has been linked to increased
210 transmissibility due to the presence of the additional basic amino acid, histidine (H). However, histidine is
211 unusual in that it has an ionizable side chain with a p*K*a near neutrality (24), and so is not conventionally

212 considered a basic amino acid. Most recently, the VOC (B.1.617.2, or Delta) has replaced B.1.1.7(Alpha) as
213 the dominant circulating virus globally, which like A.23.1 and (sub-lineages B.1.617.1 and B.1.617.3)
214 encodes a P681R substitution, and is more conventionally "polybasic" in the S1/S2 cleavage motif, than the
215 P681H of B.1.1.7 (Alpha) and is suggested to enhance transmissibility and pathogenesis (25, 26). However,
216 the A.23.1 variant pre-dated B.1.617 as a P681R-containing VOC/VOI by several months. It is important
217 to note that both lineages that have dominated Uganda have encoded the spike P681R substitution. A
218 second important detail may be the timing of position 681 changes (either to H or R) relative to other
219 changes in the spike. In all cases the position 681 change occurs after a change of position 613/614 (B to
220 B.1 to B.1.1.7, B to B.1 to B.1.617.2, and A to A.23. A.23.1 and now B to B.1 to B.1.1.7 to Q.4)
221 The analyses reported here show that the substitution strongly influences furin-mediated cleavage at the *in*
222 *vitro* level, with these results being consistent with other studies (23, 24). However, it is very clear that P681R
223 is not the sole driver of spike protein function in vivo, a finding reinforced by the molecular studies described
224 here. It would be of interest to understand associated spike changes that cooperate with P681R. The
225 introduction of P681R alone into the WT Wuhan-1 spike did not reproduce the full activity of the A.23.1
226 spike (Figures 3 and 4). One limitation of this study is that isolated viruses of the A.23.1 lineage are not
227 available for infectivity assays, and so our work relies on the use of epidemiological tools and the
228 reconstruction of virus infection in biochemical and cell-based assays. Another limitation is that our "wild-
229 type" virus contains D614 and not 614G. Despite these limitations, we consider that our data support our
230 conclusion that the spike mutation P681R—by itself—is a not a primary driver of virus transmissibility in
231 the population, with A.23.1 giving unique insight into these aspects of the ongoing COVID-19 pandemic,
232 but requires the full context of additional spike and other viral changes seen in A.23.1, B.1.617.2 and Q.4
233 for transmission success.
234 A.23.1 was a key SARS-CoV-2 variant spreading within Africa during the early part of 2021, and has been
235 defined (along with C.11) as an African VOI (27) having have multiple mutations on the spike glycoprotein
236 and evolving in a clocklike manner along with other variants. Epidemiological data from Uganda support

237 the importance of the P681R substitution in A.23.1 for community-wide transmission. The subsequent
238 decline of the P681R lineage A.23.1 in Uganda, combined with the in vitro analyses reported here clearly
239 showed that the P681R alone is not sufficient to drive such dominance. The P681R lineage B.1.617.2 (Delta)
240 likely benefited from additional S and other substitutions and eventually dominated the Uganda epidemic by
241 June 2021 (Figure 5), similar to patterns globally.
242 While P681R does make the S1/S2 cleavage site more basic in nature, such variant cleavage sites are still not
243 "ideal" for furin—as originally found in the prototype furin-cleaved virus mouse hepatitis virus (MHV)
244 (RRARR|S) (28, 29). The introduction of an arginine residue does appear to be making S1/S2 more
245 "polybasic" as the pandemic continues and transmissibility increases. While we should not over-simply the
246 complex process of spike protein activation, it will be interesting to see whether this progression of basic
247 residue addition continues with new variants, towards that seen in established community-acquired
248 respiratory (CAR) coronaviruses such as HCoV-HKU-1 or HCoV-OC43, with S1/S2 sequences of
249 RRKRR|S and RRSRR|A respectively.

250 **Acknowledgements**

251 This work was funded in part by the National Institute of Health research grant R01AI35270 (to GW and
252 SD). We thank the global SARS-CoV-2 sequencing groups for their open and rapid sharing of sequence data
253 and GISAID for providing an effective platform to make these data available. DLB, MVTP and MC were
254 funded by the UK Medical Research Council (MRC/UK Research and Innovation) and the UK Department
255 for International Development (DFID) under the MRC/DFID Concordat agreement (grant agreement no.
256 NC_PC_19060) and Wellcome Trust, UK FCDO—Wellcome Epidemic Preparedness—Coronavirus
257 (grant agreement no. 220977/Z/20/Z). TT was supported by the National Science Foundation Graduate
258 Research Fellowship Program under Grant No. DGE-1650441 and the Samuel C. Fleming Family Graduate
259 Fellowship.

260

261 **Author contributions**

Conceptualization: BL, LEF, TT, SD, JAJ and GRW. Methodology: BL, LEF, MVTP, DLB, TT, SD, MC, JAJ and GRW. Investigation: BL, LEF, MVTP, DLB, TT, JAJ. Writing - Original Draft: BL, TT, JAJ. and GRW. Writing - Review & Editing, BL, TT, SD, MC, JAJ and GRW. Visualization: BL, LEF, MVTP, TT and JAJ. Supervision: SD, MC, JAJ and G.R.W. Funding acquisition: SD, MC and GRW.

Declaration of Interests

The authors manifest no conflict of interest.

References

1. Whittaker GR, Daniel S, Millet JK. 2021. Coronavirus entry: how we arrived at SARS-CoV-2. Curr Opin Virol 47:113-120.
2. Rambaut A, Holmes EC, O'Toole A, Hill V, McCrone JT, Ruis C, du Plessis L, Pybus OG. 2020. A dynamic nomenclature proposal for SARS-CoV-2 lineages to assist genomic epidemiology. Nat Microbiol 5:1403-1407.
3. Zhou B, Thao TTN, Hoffmann D, Taddeo A, Ebert N, Labroussaa F, Pohlmann A, King J, Steiner S, Kelly JN, Portmann J, Halwe NJ, Ulrich L, Trueb BS, Fan X, Hoffmann B, Wang L, Thomann L, Lin X, Stalder H, Pozzi B, de Brot S, Jiang N, Cui D, Hossain J, Wilson MM, Keller MW, Stark TJ, Barnes JR, Dijkman R, Jores J, Benarafa C, Wentworth DE, Thiel V, Beer M. 2021. SARS-CoV-2 spike D614G change enhances replication and transmission. Nature 592:122-127.
4. Harvey WT, Carabelli AM, Jackson B, Gupta RK, Thomson EC, Harrison EM, Ludden C, Reeve R, Rambaut A, Consortium C-GU, Peacock SJ, Robertson DL. 2021. SARS-CoV-2 variants, spike mutations and immune escape. Nat Rev Microbiol doi:10.1038/s41579-021-00573-0.
5. Bugembe DL, Phan MVT, Ssewanyana I, Semanda P, Nansumba H, Dhaala B, Nabadda S, O'Toole AN, Rambaut A, Kaleebu P, Cotten M. 2021. Emergence and spread of a SARS-CoV-2 lineage A variant (A.23.1) with altered spike protein in Uganda. Nat Microbiol doi:10.1038/s41564-021-00933-9.
6. Butera Y, Mukantwari E, Artesi M, D'Arc Umuringa J, O'Toole ÁN, Hill V, Rooke S, Hong SL, Dellicour S, Majyambere O, Bontems S, Boujemla B, Quick J, Resende PC, Loman N, Umumararungu E, Kabanda A, Murindahabi MM, Tuyisenge P, Gashegu M, Rwabihama JP, Sindayiheba R, Gikic D, Souopgui J, Ndifon W, Rutayisire R, Gatare S, Mpunga T, Ngamije D, Bours V, Rambaut A, Nsanzimana S, Baele G, Durkin K, Mutesa L, Rujeni N. 2021. Genomic Sequencing of SARS-CoV-2 in Rwanda: evolution and regional dynamics. medRxiv doi:10.1101/2021.04.02.21254839:2021.04.02.21254839.
7. Bugembe DL, Phan MVT, Abias A, Ayei J, Deng LL, Lako RLL, Rumunu J, Kaleebu P, Wamala JF, Hm JJ, Lodiongo DK, Bunga S, Cotten M. 2021. SARS-CoV-2 Variants, South Sudan, January–March 2021. Emerging Infectious Disease journal 27.
8. Bugembe DL, V.T.Phan M, Ssewanyana I, Semanda P, Nansumba H, Dhaala B, Nabadda S, O'Toole ÁN, Rambaut A, Kaleebu P, Cotten M. 2021. A SARS-CoV-2 lineage A variant (A.23.1)

300 with altered spike has emerged and is dominating the current Uganda epidemic. medRxiv
301 doi:10.1101/2021.02.08.21251393:2021.02.08.21251393.

302 9. Jaimes JA, Andre NM, Chappie JS, Millet JK, Whittaker GR. 2020. Phylogenetic Analysis and
303 Structural Modeling of SARS-CoV-2 Spike Protein Reveals an Evolutionary Distinct and
304 Proteolytically Sensitive Activation Loop. J Mol Biol 432:3309-3325.

305 10. Polgár L. 1989. General Aspects of Proteases, p 43-86, Mechanisms of Protease Action. CRC
306 press, Boca Raton, FL.

307 11. Seidah NG, Prat A. 2012. The biology and therapeutic targeting of the proprotein convertases. Nat
308 Rev Drug Discov 11:367-83.

309 12. Johnson BA, Xie X, Bailey AL, Kalveram B, Lokugamage KG, Muruato A, Zou J, Zhang X,
310 Juelich T, Smith JK, Zhang L, Bopp N, Schindewolf C, Vu M, Vanderheiden A, Winkler ES,
311 Swetnam D, Plante JA, Aguilar P, Plante KS, Popov V, Lee B, Weaver SC, Suthar MS, Routh AL,
312 Ren P, Ku Z, An Z, Debbink K, Diamond MS, Shi PY, Freiberg AN, Menachery VD. 2021. Loss
313 of furin cleavage site attenuates SARS-CoV-2 pathogenesis. Nature 591:293-299.

314 13. Peacock TP, Goldhill DH, Zhou J, Baillon L, Frise R, Swann OC, Kugathasan R, Penn R, Brown
315 JC, Sanchez-David RY, Braga L, Williamson MK, Hassard JA, Staller E, Hanley B, Osborn M,
316 Giacca M, Davidson AD, Matthews DA, Barclay WS. 2020. The furin cleavage site of SARS-CoV-
317 2 spike protein is a key determinant for transmission due to enhanced replication in airway cells.
318 bioRxiv doi:10.1101/2020.09.30.318311:2020.09.30.318311.

319 14. Hoffmann M, Kleine-Weber H, Schroeder S, Kruger N, Herrler T, Erichsen S, Schiergens TS,
320 Herrler G, Wu NH, Nitsche A, Muller MA, Drosten C, Pohlmann S. 2020. SARS-CoV-2 Cell
321 Entry Depends on ACE2 and TMPRSS2 and Is Blocked by a Clinically Proven Protease Inhibitor.
322 Cell 181:271-280 e8.

323 15. Lubinski B, Tang T, Daniel S, Jaimes JA, Whittaker GR. 2021. Functional evaluation of proteolytic
324 activation for the SARS-CoV-2 variant B.1.1.7: role of the P681H mutation. bioRxiv
325 doi:10.1101/2021.04.06.438731.

326 16. Tian S, Huajun W, Wu J. 2012. Computational prediction of furin cleavage sites by a hybrid
327 method and understanding mechanism underlying diseases. Sci Rep 2:261.

328 17. Duckert P, Brunak S, Blom N. 2004. Prediction of proprotein convertase cleavage sites. Protein
329 Eng Des Sel 17:107-12.

330 18. Jaimes JA, Millet JK, Whittaker GR. 2020. Proteolytic Cleavage of the SARS-CoV-2 Spike Protein
331 and the Role of the Novel S1/S2 Site. iScience 23:101212.

332 19. Millet JK, Tang T, Nathan L, Jaimes JA, Hsu HL, Daniel S, Whittaker GR. 2019. Production of
333 Pseudotyped Particles to Study Highly Pathogenic Coronaviruses in a Biosafety Level 2 Setting. J
334 Vis Exp doi:10.3791/59010.

335 20. Muller NF, Wagner C, Frazar CD, Roychoudhury P, Lee J, Moncla LH, Pelle B, Richardson M,
336 Ryke E, Xie H, Shrestha L, Addetia A, Rachleff VM, Lieberman NAP, Huang ML, Gautom R,
337 Melly G, Hiatt B, Dykema P, Adler A, Brandstetter E, Han PD, Fay K, Ilcisin M, Lacombe K,
338 Sibley TR, Truong M, Wolf CR, Boeckh M, Englund JA, Famulare M, Lutz BR, Rieder MJ,
339 Thompson M, Duchin JS, Starita LM, Chu HY, Shendure J, Jerome KR, Lindquist S, Greninger
340 AL, Nickerson DA, Bedford T. 2021. Viral genomes reveal patterns of the SARS-CoV-2 outbreak
341 in Washington State. Sci Transl Med 13.

342 21. Richard D, Shaw LP, Lanfear R, Acman M, Owen CJ, Tan CC, van Dorp L, Balloux F. 2021. A
343 phylogeny-based metric for estimating changes in transmissibility from recurrent mutations in
344 SARS-CoV-2. bioRxiv doi:10.1101/2021.05.06.442903:2021.05.06.442903.

345 22. Grubaugh ND, Hodcroft EB, Fauver JR, Phelan AL, Cevik M. 2021. Public health actions to
346 control new SARS-CoV-2 variants. Cell 184:1127-1132.

347 23. Peacock TP, Penrice-Randal R, Hiscox JA, Barclay WS. 2021. SARS-CoV-2 one year on: evidence
348 for ongoing viral adaptation. J Gen Virol 102.

349 24. Nelson DL, Cox MM. 2000. Lehninger Principles of Biochemistry. Worth Publishers.

350 25. Peacock TP, Sheppard CM, Brown JC, Goonawardane N, Zhou J, Whiteley M, de Silva TI, Barclay
351 WS. 2021. The SARS-CoV-2 variants associated with infections in India, B.1.617, show enhanced
352 spike cleavage by furin. bioRxiv doi:10.1101/2021.05.28.446163:2021.05.28.446163.

353 26. Saito A, Nasser H, Uriu K, Kosugi Y, Irie T, Shirakawa K, Sadamasu K, Kimura I, Ito J, Wu J,
354 Ozono S, Tokunaga K, Butlertanaka EP, Tanaka YL, Shimizu R, Shimizu K, Fukuhara T,
355 Kawabata R, Sakaguchi T, Yoshida I, Asakura H, Nagashima M, Yoshimura K, Kazuma Y,
356 Nomura R, Horisawa Y, Takaori-Kondo A, Nakagawa S, Ikeda T, Sato K. 2021. SARS-CoV-2
357 spike P681R mutation enhances and accelerates viral fusion. bioRxiv
358 doi:10.1101/2021.06.17.448820:2021.06.17.448820.

359 27. Wilkinson E, Giovanetti M, Tegally H, San JE, Lessels R, Cuadros D, Martin DP, Zekri A-RN,
360 Sangare AK, Ouedraogo A-S, Sesay AK, Hammami A, Amuri AA, Sayed A, Rebai A, Elargoubi A,
361 Trotter AJ, Keita AK, Sall AA, Kone A, Souissi A, Gutierrez AV, Page AJ, Iranzadeh A, Lambisia
362 A, Sylverken A, Ibrahimi A, Dhaala B, Kouriba B, Kleinhans B, Brook C, Williamson C, Pratt CB,
363 Akoua-Koffi CG, Agoti CN, Morang'a CM, Nokes DJ, Bridges DJ, Bugembe DL, Baker D,
364 Doolabh D, Ssemwanga D, Tshabuila D, Bassirou D, Amuzu DSY, Goedhals D, Maruapula D,
365 Foster-Nyarko E, Lusamaki EK, Simulundu E, et al. 2021. A year of genomic surveillance reveals
366 how the SARS-CoV-2 pandemic unfolded in Africa. medRxiv
367 doi:10.1101/2021.05.12.21257080:2021.05.12.21257080.

368 28. Sturman LS, Ricard CS, Holmes KV. 1985. Proteolytic cleavage of the E2 glycoprotein of murine
369 coronavirus: activation of cell-fusing activity of virions by trypsin and separation of two different
370 90K cleavage fragments. J Virol 56:904-11.

371 29. Whittaker GR. 2021. SARS-CoV-2 spike and its adaptable furin cleavage site. Lancet Microbe
372 2:e488-e489.

373 30. Sun X, Tse LV, Ferguson AD, Whittaker GR. 2010. Modifications to the hemagglutinin cleavage
374 site control the virulence of a neurotropic H1N1 influenza virus. J Virol 84:8683-90.

375

376

377 **Methodology**

378 **Furin prediction calculations.** Prop: CoV sequences were inputted into the ProP 1.0 Server hosted at:
379 cbs.dtu.dk/services/ProP/ PiTou: CoV sequences were analyzed using the PiTou V3 software hosted at:
380 http://www.nuolan.net/reference.html.

381

382 **Fluorogenic peptide assays**

383 Fluorogenic peptide assays were performed as described previously with minor modifications (18). Each
384 reaction was performed in a 100 µl volume consisting of buffer, protease, and SARS-CoV-2 S1/S2 Wuhan-
385 Hu-1 (WT) (TNSPRRARSVA), SARS-CoV-2 S1/S2 B.1.1.7 (TNSHRRARSVA) or SARS-CoV-2 S1/S2
386 A.23.1 (TNSRRRARSVA) fluorogenic peptide in an opaque 96-well plate. For trypsin catalyzed reactions,
387 0.8 nM/well TPCK trypsin was diluted in PBS buffer. For furin catalyzed reactions, 1 U/well recombinant
388 furin was diluted in a buffer consisting of 20 mM HEPES, 0.2 mM $CaCl_2$, and 0.2 mM β-mercaptoethanol,
389 at pH 7.5. Fluorescence emission was measured once per minute for 60 continued minutes using a
390 SpectraMax fluorometer (Molecular Devices) at 30°C with an excitation wavelength of 330 nm and an
391 emission wavelength of 390 nm. Vmax was calculated by fitting the linear rise in fluorescence to the equation
392 of a line.

393

394 **Synthesis and cloning of the A.23.1 spike protein**

395 The sequence for the A.23.1 spike gene from isolate SARS-CoV-2 A.23.1 hCoV-19/Uganda/UG185/2020
396 (EPI_ISL_955136) was obtained from GISAID (https://www.gisaid.org/), codon-optimized, synthesized
397 and cloned into a pcDNA 3.1+ vector for expression (GenScript). line.

398

399 **Site-directed Mutagenesis**

400 Primers (ACCTGGCTCTCCTTCGGGAGTTTGTCTGG/CCAGACAAACTCCCGAAGGAGAGCCAGGT)
401 for mutagenesis were designed using the Agilent QuickChange Primer Design tool to create the P681R
402 mutation (CCA->CGA). Mutagenesis was carried out on a pCDNA-SARs2 Wuhan-Hu-1 S plasmid using
403 the Agilent QuickChange Lightning Mutagenesis kit (The original plasmid was generously provided by David
404 Veesler, University of Washington USA). The mutated pcDNA-SARS-CoV-2 Wuhan-Hu-1 P681R S
405 plasmid was used to transform XL-10 gold ultracompetent cells, which were grown up in small culture, and

406 then plasmid was extracted using the Qiagen QIAprep Spin Miniprep Kit. Sanger Sequencing was used to
407 confirm incorporation of the mutation.
408
409 **Cell-to-cell fusion assay**
410 Vero E6 and Vero-TMPRSS2 cells were transfected with a plasmid harboring the spike gene of the SARS-
411 CoV-2 Wuhan-Hu-1 S (WT), SARS-CoV-2 A.23.1 S, SARS-CoV-2 Wuhan-Hu-1 with a P to R mutation in
412 the 681 amino acid position (P681R), or a delta-spike pCDNA3.1+ (S-) plasmid, and evaluated through an
413 immunofluorescence assay (IFA), nuclei involved in syncytia counting, cell-to-cell fusion ratio and western
414 blot. Transfection was performed on 8-well glass slides at 90% confluent cells using Lipofectamine® 3000
415 (Cat: L3000075, Invitrogen Co.), following the manufacturer's instructions and 250 ng of plasmid DNA per
416 well were transfected. Cells were then incubated at 37°C with 5% of CO_2 for 28 hours. Syncytia was
417 visualized through fluorescence microscopy using a previously described method (15). The spike expression
418 was detected using a SARS-CoV-2 spike antibody (Cat: 40591-T62, Sino Biological Inc.) at 1/500 dilution
419 for 1 hour. Secondary antibody labeling was performed using AlexaFluor™ 488 goat anti-rabbit IgG
420 antibody (Cat: A32731, Invitrogen Co.) at a 1/500 dilution for 45 minutes. Representative images of each
421 treatment group were taken, and these images were used to calculate the percent of nuclei involved in the
422 formation of syncytia and for quantification of the cell-to-cell fusion ratio based in fluorescence intensity.
423 Images were taken at 20X on the Echo Revolve fluorescent microscope (Model: RVL-100-M). The nuclei
424 were counted manually using the Cell Counter plugin in ImageJ (https://imagej.nih.gov/ij/). Cells that
425 expressed the spike protein and contained 4 or more nuclei were considered to be one syncytium. Cell-to-
426 cell fusion ration was calculated using image J version 1.53 (National Institutes of Health). Expressed protein
427 from Vero E6 and Vero-TMPRSS2 cells was analyzed through a cell surface biotinylation assay western blot
428 as described previously. (30) Spike protein was detected using the antibodies described previously in this
429 section. GLUT4 protein was used as a housekeeping expression control and labeled using a GLUT4
430 monoclonal antibody (Cat: MA5-17175, Invitrogen Co.).

431

432 **Pseudoparticle Generation**

433 Pseudoparticle generation was carried out using a murine leukemia virus (MLV)-based system as previously
434 described with minor modification (19). HEK293T cells were seeded at $2.5x10^5$ cells/ml in a 6-well plate the
435 day before transfection. Transfections were performed using polyethylenimine (PEI) and 1X Opti-Mem
436 from Gibco. Cells were transfected with 800 ng of pCMV-MLV-gagpol, 600 ng of pTG-luc, and 600 ng of
437 a plasmid containing the viral envelope protein of choice. Viral envelope plasmids included pcDNA-SARS-
438 CoV-2 Wuhan-Hu1 S as the WT, pcDNA-SARS-CoV-2 Wuhan-Hu-1 P681R S, and pcDNA-SARS-CoV-2
439 A.23.1 S. pCAGGS-VSV G was used as a positive control and pCAGGS was used for a Δ-envelope negative
440 control. At 48 hours post-transfection, the supernatant containing the pseudoparticles was removed,
441 centrifuged to remove cell debris, filtered, and stored at -80°C.

442

443 **Pseudoparticle Infection Assay**

444 Infection assays were performed as previously described with minor adjustments (19). Vero E6 and Vero-
445 TMPRSS2 cells were seeded at $4.5x10^5$ cells/ml in a 24-well plate the day before infection. Calu-3 cells were
446 seeded at 10 $x10^5$ cells/ml in a 24-well plate three days before infection. Cells were washed three times with
447 DPBS and infected with 200 µl of either VSV G, SARS-CoV-2 S, SARS-CoV-2 P681R S, SARS-CoV-2
448 A.23.1 S, or Δ-envelope pseudoparticles. Infected cells incubated on a rocker for 1.5 hours at 37°C, and then
449 300 µl of complete media was added and cells were left at 37°C. At 72 hours post-infection, cells were lysed
450 and the level of infection was assessed using the Promega Luciferase Assay System. The manufacturer's
451 protocol was modified by putting the cells through 3 freeze/thaw cycles after the addition of 100 µl of the
452 lysis reagent. 10 µl of the cell lysate was added to 20 µl of luciferin, and then luciferase activity was measured
453 using the Glomax 20/20 luminometer (Promega). Vero E6 and Vero-TMPRSS2 infection assays were
454 replicated four times. The Calu-3 infection assays were replicated three times. Each assay was performed as
455 technical replicates, with the same batch of pseudoparticles used for all of data.

456

457 **Western blot analysis of pseudoparticles**. A 3 ml volume of pseudoparticles was pelleted using a TLA-
458 55 rotor with an Optima-MAX-E ultracentrifuge (Beckman Coulter) for 2 hours at 42,000 rpm at 4°C.
459 untreated particles were resuspended in 30 µl DPBS buffer. For the + furin treated MLVpps, particles were
460 resuspended in 30 µL of furin buffer consistent in 20 mM HEPES, 0.2 mM CaCl2, and 0.2 mM β-
461 mercaptoethanol (at pH 7.0). Particles were later incubated with 6 U of recombinant furin for 3 h at 37 °C.
462 Sodium dodecyl sulfate (SDS) loading buffer and DTT were added to samples and heated at 65°C for 20
463 minutes. Samples were separated on NuPAGE Bis-Tris gel (Invitrogen) and transferred on polyvinylidene
464 difluoride membranes (GE). SARS-CoV-2 S was detected using a rabbit polyclonal antibody against the S2
465 domain (Cat: 40590-T62, Sinobiological) and an AlexaFluor 488 goat anti-rabbit antibody. Bands were
466 detected using the ChemiDoc Imaging software (Bio-Rad) and band intensity was calculated using the
467 analysis tools on Biorad Image Lab 6.1 software to determine the uncleaved to cleaved S ratios.

468

469 **Uganda cases vs. viral lineages over time.** Daily reported SARS-CoV-2 infections The Uganda daily
470 SARS-CoV-2 positive samples numbers were retrieved from Our World in Data
471 (https://ourworldindata.org/coronavirus) and the 7 day average was determined. Uganda SARS-CoV-2
472 lineage data were generated from the MRC Uganda genomic data deposited in the GISAID database
473 (https://www.gisaid.org/). SARS-CoV-2 Pango lineages (2) were determined using the pangolin module
474 pangoLEARN (https://github. com/cov-lineages/pangolin).

475

476 **Spike position 681 and 613/614 changes in global data.** All available spike protein sequences were
477 obtained from the GISAID database. The frequency of P681, P681R, P681H, D614 D614G and D613H
478 were counted by string matching using Ack (http://beyondgrep.com/) to the major variations of the 88
479 amino acid peptide sequence (aa 605 to 691) spanning the two relevant sites (D614_P681 (Wuhan_B),
480 D614G_P681 (B.1), D614_P681H, D614G_P681H (B.1.1.7), D614_P681R, Q613_P681 (Wuhan_B),

481 Q613H_P681 (A.23), Q613H_P681R (A.23.1), D614G_P681R (B.1.617.2). Fractions of available total
482 genomes for each month encoding each peptide variant were visualized in a heatmap. Additional changes at
483 position H655Y (present in the Gamma lineage) were also included in the count and fraction calculation but
484 the total numbers were minor.
485
486
487
488
489
490
491
492
493

A

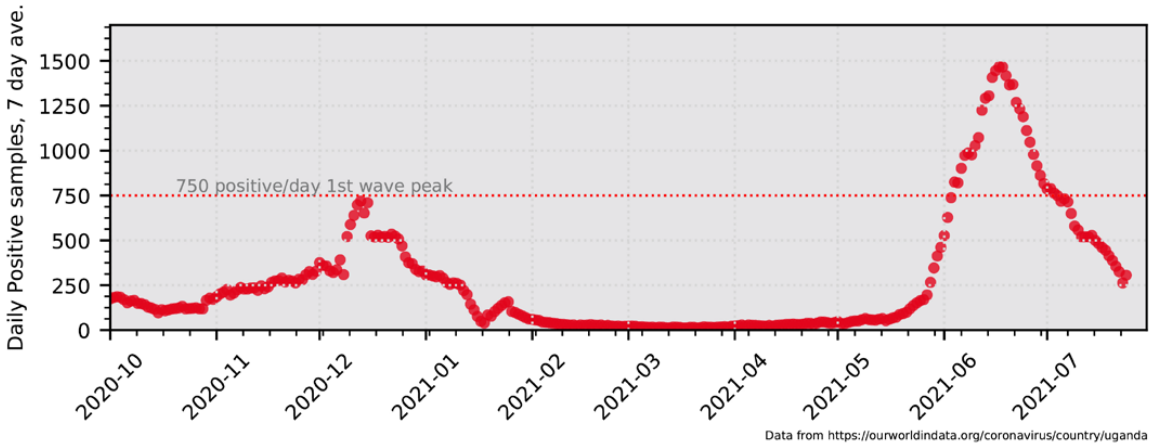

B

Lineage	Oct-20	Nov-20	Dec-20	Jan-21	Feb-21	Mar-21	Apr-21	May-21	Jun-21	Jul-21
A.23.1	0.14	0.42	0.88	1	0.4	0.2	0.21	0.07	0.02	0
A.23	0.24	0.3	0.05	0	0.05	0	0	0	0	0
A	0.1	0	0	0	0	0	0	0	0	0
A.19	0	0	0	0	0	0	0.03	0	0	0
A.25	0	0.03	0.01	0	0	0	0	0	0	0
B	0	0	0	0	0	0	0	0	0	0
B.1	0.1	0.03	0.02	0	0	0	0	0	0	0
B.1.1	0	0	0	0	0	0	0.03	0	0	0
B.1.1.161	0	0	0.01	0	0	0	0	0	0	0
B.1.1.27	0.29	0	0	0	0	0	0	0	0	0
B.1.1.318	0	0	0	0	0.15	0	0.03	0	0	0
B.1.214	0.05	0.03	0	0	0	0	0	0	0	0
B.1.222	0	0.03	0.02	0	0.1	0	0	0	0	0
B.1.363	0	0.03	0	0	0	0	0	0	0	0
B.1.393	0.1	0.12	0	0	0	0	0	0	0	0
B.1.351	0	0	0	0	0.2	0.25	0.1	0	0.02	0
B.1.1.7	0	0	0	0	0	0.28	0.03	0.14	0.01	0
B.1.617.1	0	0	0	0	0	0.03	0	0	0	0
B.1.525	0	0	0	0	0.1	0.25	0.41	0.57	0.01	0
B.1.617.2	0	0	0	0	0	0	0.14	0.21	0.95	1

Month

Figure 1: Global frequency of furin site substitutions. The frequency of P681, P681R, P681H, D614 D614G and D613H substitutions were counted by string matching to a peptide sequencing spanning the position 613 to 681) including the relevant sites at 613/614 and 681. (D614_P681 (Wuhan_B), D614G_P681 (B.1), D614_P681H, D614G_P681H (B.1.1.7), D614_P681R, Q613_P681 (Wuhan_B), Q613H_P681 (A.23), Q613H_P681R (A.23.1), D614G_P681R (B.1.617.2). Fractions of total genomes available for each month were plotted. Color bar at the bottom of each panel indicate fraction/color code. Panel A. Lineage B relevant substitutions. Panel B. Lineage A.23 and A.23.1 relevant substitutions.

A

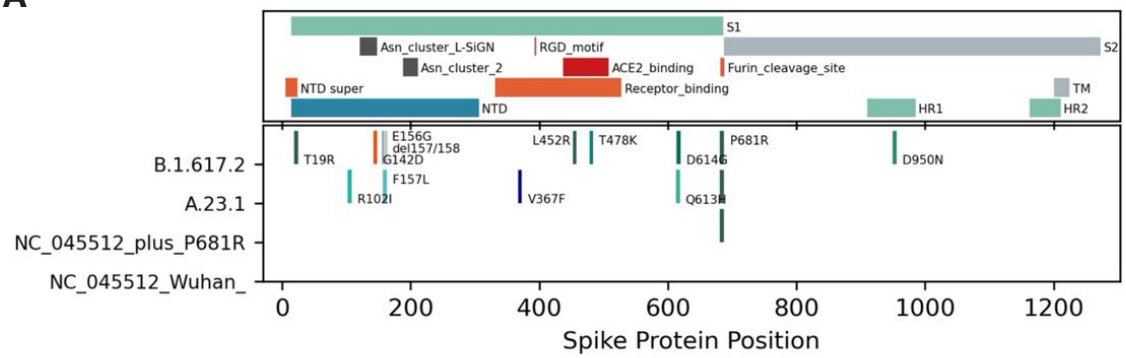

B

Virus	S1/S2 Sequence	Furin Score PiTou	Furin Score ProP
SARS-CoV-2 (A.1/B.1)	672-ASYQTQTNSPRRAR|SVASQS-691	+9.196	0.626
SARS-CoV-2 (B.1.1.7)	669-ASYQTQTNSHRRAR|SVASQS-688	+9.907	0.706
SARS-CoV-2 (A.23.1)	669-ASYQTQTNSRRRAR|SVASQS-688	**+12.209**	**0.704**
SARS-CoV-2 (B.1.617.2)	669-ASYQTQTNSRRRAR|SVASQS-688	+12.209	0.704
MERS-CoV	738-LPDTPSTLTPRSVR|SVPGEM-757	+5.155	0.556
HCoV-HKU1	747-YNSPSSSSSRRKRR|SISASY-766	+14.634	0.868
HCoV-OC43 (clinical)	750-GYCVDYFKNRRSRR|AITTGY-769	+10.10	0.736

C

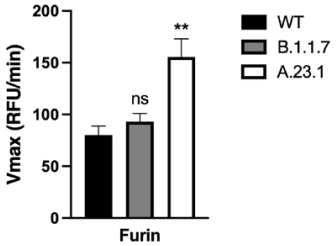

Figure 2: A. Summary of notable functional domains and sequence changes in the spike gene of A.23.1 compared to Wuhan-Hu-1 and B.1.617.2 (Delta). **B.** Furin cleavage score analysis of CoV S1/S2 cleavage sites. CoV S sequences were analyzed using the ProP1 1.0 and PiTou2 3.0 furin prediction algorithm, generating a score with bold numbers indicating predicted furin cleavage. (|) denotes the position of the predicted S1/S2 cleavage site. Basic resides, arginine (R) and lysine (K), are highlighted in blue, with histidine in purple. Sequences corresponding to the S1/S2 region of SARS-CoV-2 (QHD43416.1), SARS-CoV (AAT74874.1), MERS-CoV (AFS88936.1), HCoV-HKU1 (AAT98580.1), HCoV-OC43 (KY369907.1) were obtained from GenBank. Sequences corresponding to the S1/S2 region of SARS-CoV-2 B.1.1.7 (EPI_ISL_1374509) and SARS-CoV-2 A.23.1 hCoV-19/Uganda/UG185/2020 (EPI_ISL_955136), were obtained from GISAID. **C.** Fluorogenic peptide cleavage assays of the SARS-CoV-2 S1/S2 cleavage site. Peptides mimicking the S1/S2 site of the SARS-CoV-2 Wuhan-Hu-1 (WT – P681), B.1.1.7 (P681H) and A.23.1 (P681R) variants were evaluated for in vitro cleavage by furin, compared to trypsin control.

A

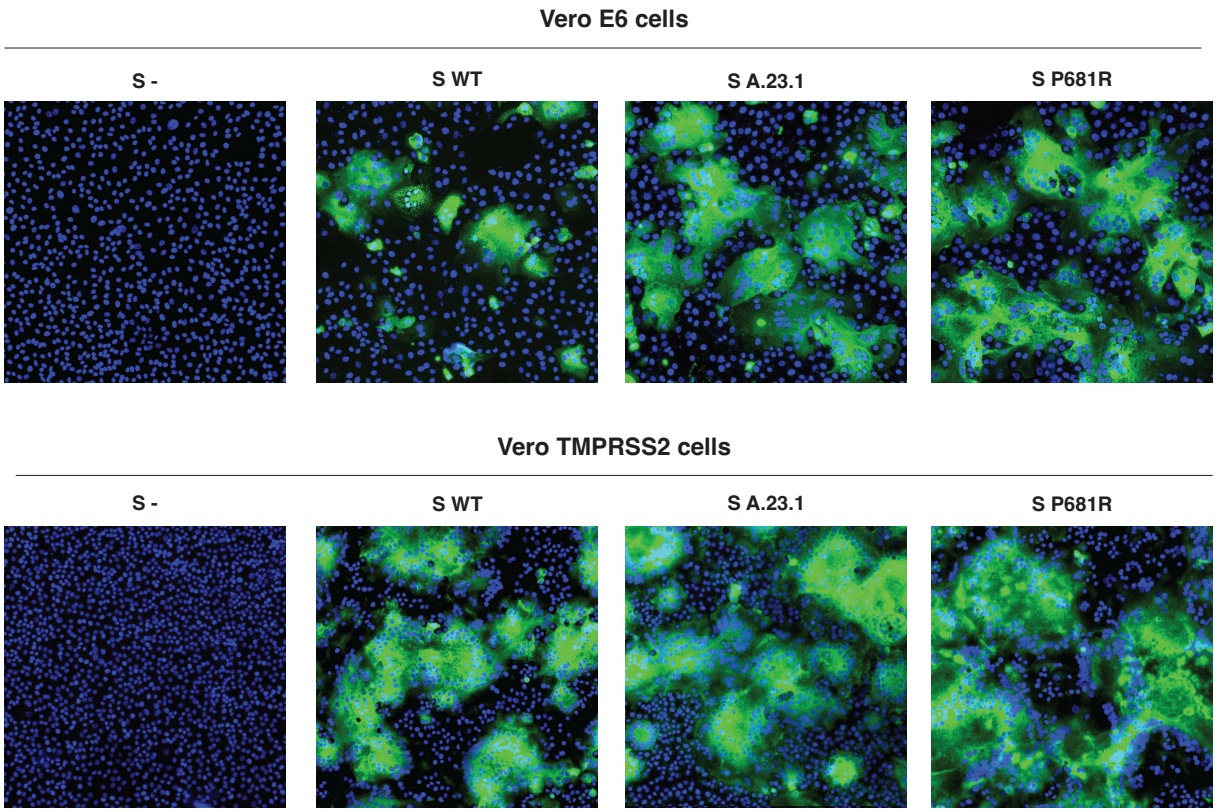

B

Vero E6 cells			
	# Total nuclei	# Nuclei involved in syncytia	% Nuclei involved in syncytia
S -	6,824	0	0
S WT	4,866	345	7.09
S A.23.1	4,627	1054	22.77
S P681H	4,703	955	20.30

Vero-TMPRSS2 cells			
	# Total nuclei	# Nuclei involved in syncytia	% Nuclei involved in syncytia
S -	13,051	0	0
S WT	10,441	7718	73.92
S A.23.1	7,861	6367	80.99
S P681H	10,747	8033	74.74

C

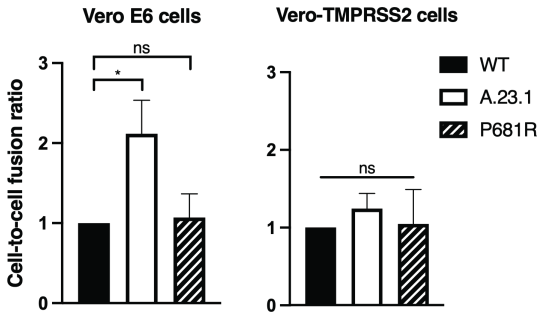

D

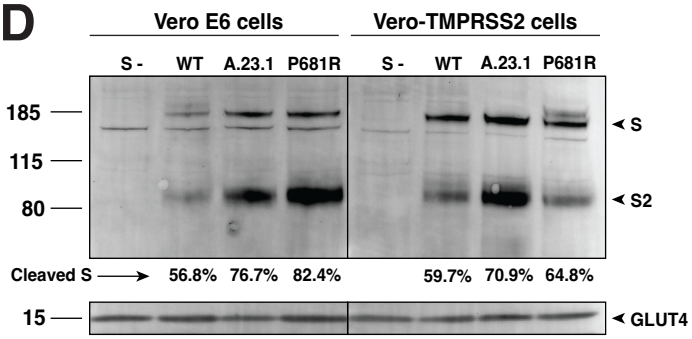

Figure 3: A. Cell-to-cell fusion assay of SARS-CoV-2 Wuhan-Hu-1 S (WT), SARS-CoV-2 S A.23.1 variant, or SARS-CoV-2 S WT with P681R mutation. S- = non-transfected cells. SARS-CoV-2 S was detected using a rabbit antibody against the SARS-CoV-2 S2 region. **B.** Syncytia quantification by number of nuclei involved in syncytia. **C.** Cell-to-cell fusion ratio measured by fluorescence intensity. **D.** Western blot analysis of membrane expressed S proteins and GLUT4 (housekeeping expression protein). All the experiments were performed on Vero E6 and Vero-TMPRSS2 cells.

536

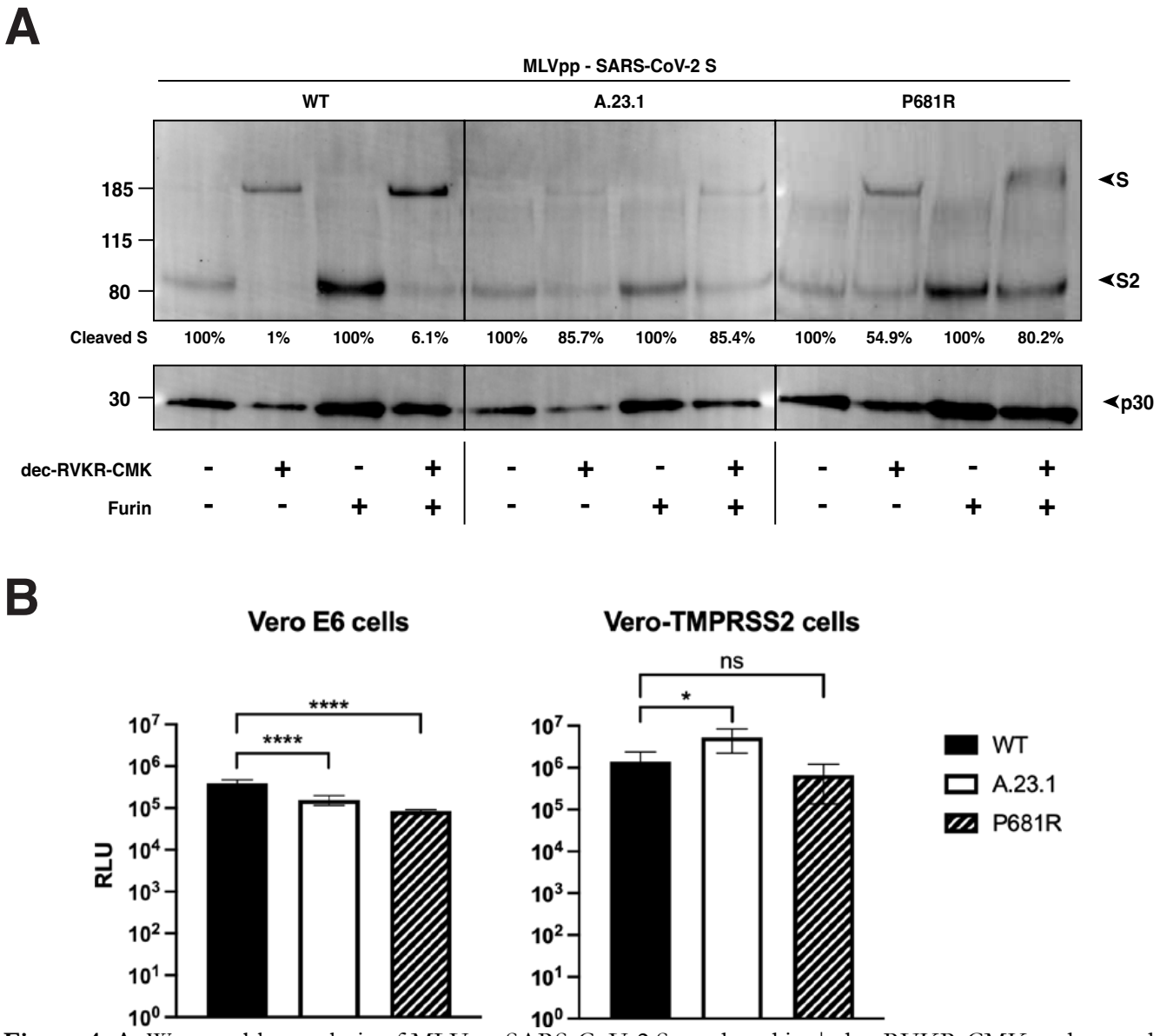

537
538 **Figure 4: A.** Western blot analysis of MLVpp-SARS-CoV-2 S produced in ± dec-RVKR-CMK and treated
539 with ± furin. S was detected using a rabbit antibody against the SARS-CoV-2 S2 subunit. MLV content was
540 detected using a mouse antibody against MLV p30. **B.** Pseudoparticle infectivity assays in Vero E6, Vero-
541 TMPRSS2 or Calu-3 cells. Cells were infected with MLVpps harboring the VSV-G, SARS-CoV-2 S (WT),
542 SARS-CoV-2 S A.23.1 variant, SARS-CoV-2 S WT with P681R mutation. Data represents the average
543 luciferase activity of cells of three (Vero E6 and Vero-TMPRSS2).
544

545

546

547

548

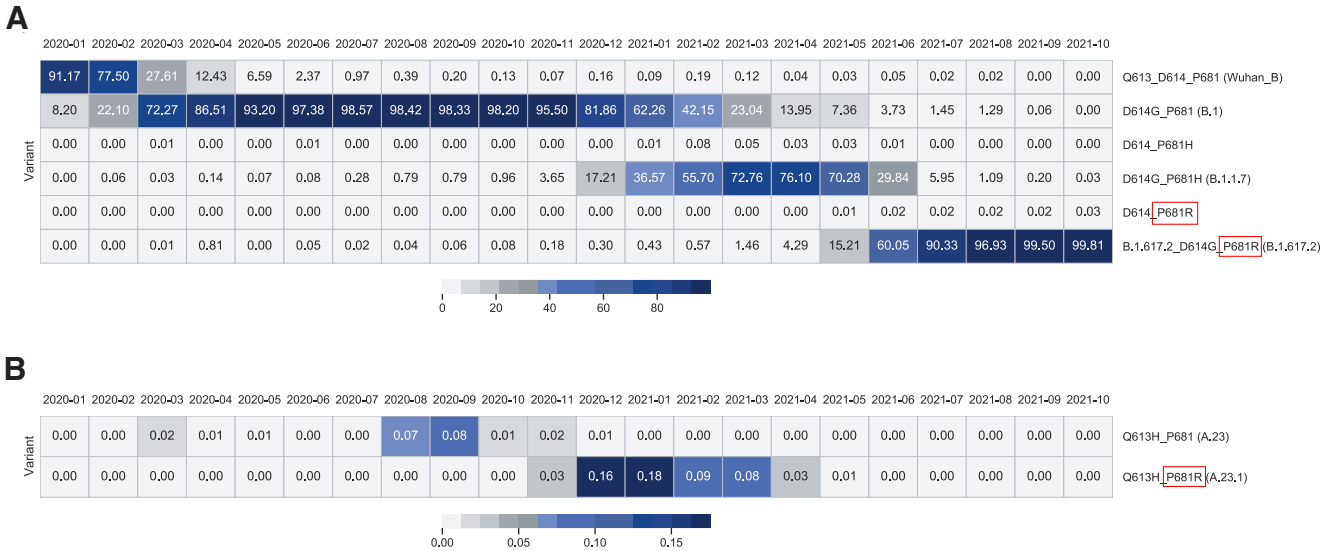

Figure 5: Uganda SARS-CoV-2 cases and lineages, October 2020 to June 2021. **A.** 7-day average positive cases numbers were plotted by day, the peak of 750 cases/ per day observed in the first wave of infections in January 2021 is indicated with a dotted line. Case data were obtained from Our World in Data (https://ourworldindata.org/). **B.** Monthly SARS-CoV-2 lineage data for Uganda. All Uganda full genome sequences from GISAID (https://www.gisaid.org/) were retrieved, lineage types using the Pango tool (https://cov-lineages.org/resources/pangolin.html), and the fraction of each month's total genomes were plotted. Fractions were indicated in each cell and cells are colored (white to dark red) by increasing fraction.